Supporting Information

Efficient electronic transport in partially disordered Co_3O_4 nanosheets for electrocatalytic oxygen evolution reaction

Lejing Li,[†] *Zhuofeng Hu,*[‡] *Li Tao,*[§] *Jianbin Xu,*[§] *Jimmy C. Yu*,*[†]

[†] Department of Chemistry, The Chinese University of Hong Kong, Hong Kong SAR, China

[‡] School of Environmental Science and Engineering, Sun Yat-Sen University, Guangzhou 510006, China.

[§] Department of Electronic Engineering, The Chinese University of Hong Kong, Hong Kong SAR, China

Corresponding Author

jimyu@cuhk.edu.hk

1 Experimental Section

1.1 Electrodes preparation

These three electrodes were prepared by electrodepositing Co- and Ce-nitrate precursor onto a piece of nickel foam (NF) at 25 ^{o}C in a 40 mL electrolytic bath, NF (NF, 1 cm ×2 cm), carbon rod and saturated calomel electrode (SCE) served as the working, counter and reference electrode, respectively. Before deposition, the NF was cleaned in 6 M HCl ultrasonically to remove the oxide layer. In a typical synthesis, the NF was applied to a cathodic deposition at -1 V vs SCE in electrolyte (20 mM cobalt nitrate and 50 mM ammonium nitrate) for 20 min to obtain the precursor film for NF/Co_3O_4 electrode. And layer of ceria was further electrodeposited on to above electrode in 10 mM cerium nitrate at -0.84 V vs SCE for 3 minutes to obtain the precursor film for NF/Co_3O_4-CeO_2 electrode. To obtain the precursor film for NF/$Co_{3-x}Ce_xO_4$, the electrolyte contains 20 mM total metal ions with different Co to Ce ratio. The NF/$Co_{3-x}CeO_4$ with the best OER performance was electrodeposited from a precursor with molar ratio of Co:Ce = 20:1. All as-prepared precursor films was subsequently heated at 300^{o}C for 2 hours to obtain the final electrodes. During the electrodeposition process, nitrate ions are reduced to ammonium ions and hydroxide ions, increasing the local pH near the NF surface then inducing the deposition of cobalt and cerium ions.

1.2 Characterization measurements

The phases on the NFs were examined using X-ray Diffraction (XRD) (Rigaku SmartLab X-ray diffractometer) with Cu Kα irradiation (λ =1.5406Å) operating at 40 kV and 40 mV. Scanning electron microscopy (SEM) was recorded by an FEI Quanta 400 microscope. Transmission electron microscopy (TEM), high-resolution TEM, the selected area electron diffraction (SAED) patterns and energy dispersive X-ray spectrometry (EDX) were performed by a Philips Tecnai F20 instrument and a CM-120 microscope (Philips, 120 kV), High-angle annular dark-field (HADDF) TEM was conducted on FEI Tecnai G2 F30 operated at 300 kV. *In situ* Raman test for powder catalysts was conducted in a homemade electrochemical cell under controlled potentials. All Raman data were recorded by HORIBA LabRAM HR Evolution Raman system with an excitation wavelength of 532 nm. X-Ray photoelectron spectroscopy (XPS) was performed using a Thermo ESCALAB 250Xi spectrometer equipped

with an anode of Al Kα radiation (1486.6 eV) X-ray sources and the result is calibrated by C1s (284.8 eV). The inductively coupled plasma atomic emission spectrometric measurements were conducted to determine the molar ratio of Ce and Co by an ICP-Prodigy7 analyzer (Teledyne Leeman Labs). A commercial differential electrochemical mass spectrometry (DEMS, Hiden HPR-40) was used to record the volatile products. We use PTFE membrane (cobetter, PF-002HS) to separate the volatile products from electrolyte. The atomic force microscopy (AFM) was performed by ScanAsyst mode with a Dimension Icon system in air.

1.3 Electrochemistry test

All OER activity, stability, and electrochemical active area (ECSA) measurements in 1 M KOH potassium hydroxide electrolyte was carried out with CHI 760D electrochemical station (CH Instruments, Inc., Shanghai) in a three-electrode set-up, consisting of each OER electrode as the working electrode, a carbon rod as counter electrode and Hg/HgO as reference electrode. LSV measurements were conducted in O_2 saturated electrolyte at a scan rate of 5 mV s^{-1}. Catalyst ink dispersions used to dropcast onto glass carbon disc were prepared before, briefly, this involved placing 2.0 mg catalyst, 1 mL deionized water, 0.5 mL isopropanol solution, and 5 uL 5wt% Nafion into a vial. The mixture was sonicated for 20 min, then 10 uL ink was dropcast onto a GC disc and dried at room temperature. For the ECSA measurements, the potential was cycled between 0.85 V and 0.95 V vs RHE where there is non-faradaic current at different scan rates (5, 10, 15, 20 and 25 mV s^{-1}). The current values recorded at 0.895 V vs RHE with different scan rates were used to determine the ECSA as the slope of the plot of current versus scan rate. The faradaic efficiency was calculated by the total amount of oxygen and the total charge passed through the electrolytic cell. The quantification of oxygen evolved was measured by a drainage method in a gas-tight H-cell. The O_2 evolution activity at two different time scales was investigated by drainage method and DEMS (5 minutes). The electrochemical impedance (EIS) of electrodes were tested by SP-200 potentiostat/EIS (BioLogic Science Instrument), a frequency window between 0.01 Hz and 100 kHz was chosen to test the impedance of electrodes with 5 mV amplitude about the open-circuit potential. The C_{dl} of each catalyst is determined from CV curves in same potential range under differ scan rates. Firstly, linear simulation of current values at each sweep speed. Then the slope of

simulated line can deduce ECSA (ECSA=C_{dl}/C_s). C_s is the specific capacitance of catalyst with a constant value, normally 40 mF cm^{-2} is used.[1, 2]

The turnover frequency is calculated by the following formula:

$$\mathrm{TOF} = \frac{j \times \mathrm{A}}{\mathrm{n} \times \mathrm{F} \times N_s}$$

where j is the current density at overpotential of 270 mV, A is the area of actual electrode, n is 4 for the electron transferred for OER, F is the Faraday constant (96485 C mol^{-1}) and N_s is the concentration of active site that is electrochemically active. Here, the N_s was the number of metal ions determined by ICP analysis.[3]

2 Additional Data and Figures

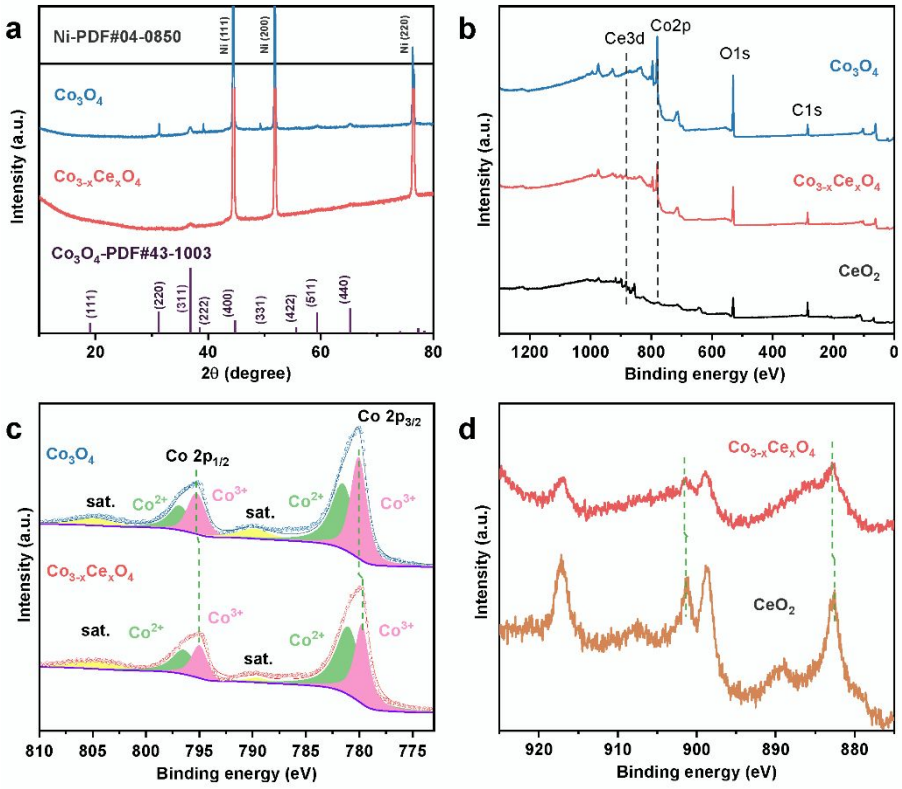

Figure S1. (a) XRD patterns and (b) XPS full spectrum of spinel Co_3O_4 and $Co_{3-x}Ce_xO_4$ (Co/Ce=13:1) supported on NF. High-resolution XPS spectrum of (c) Co 2p, and (d) Ce 3d for both samples scraped from nickel foam. Note: The CeO_2 sample in (d) was conducted by similar method to $Co_{3-x}Ce_xO_4$ without cobalt precursor added.

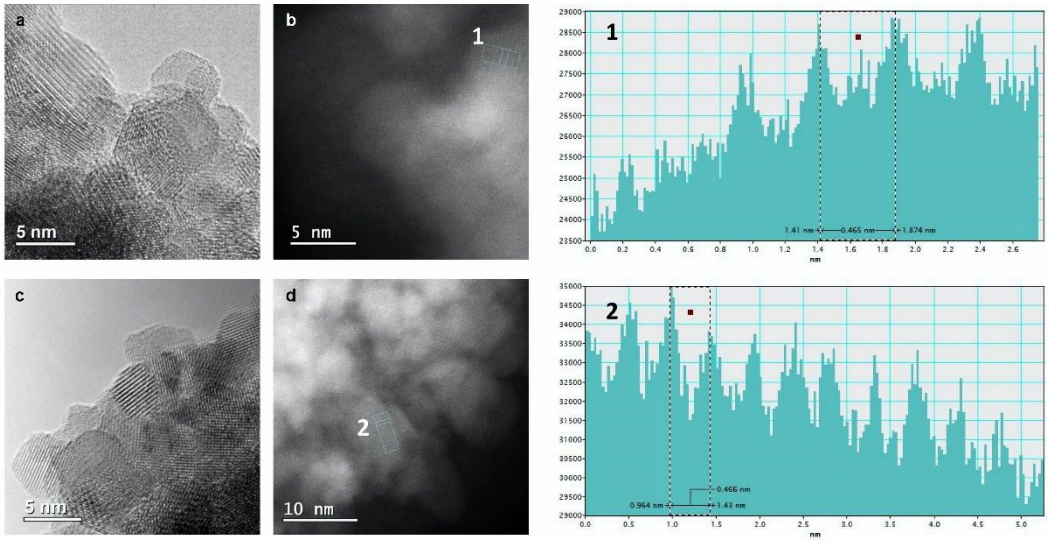

Figure S2. (a, c) HRTEM and (b, d) HADDF-TEM images for sample $Co_{3-x}Ce_xO_4$.

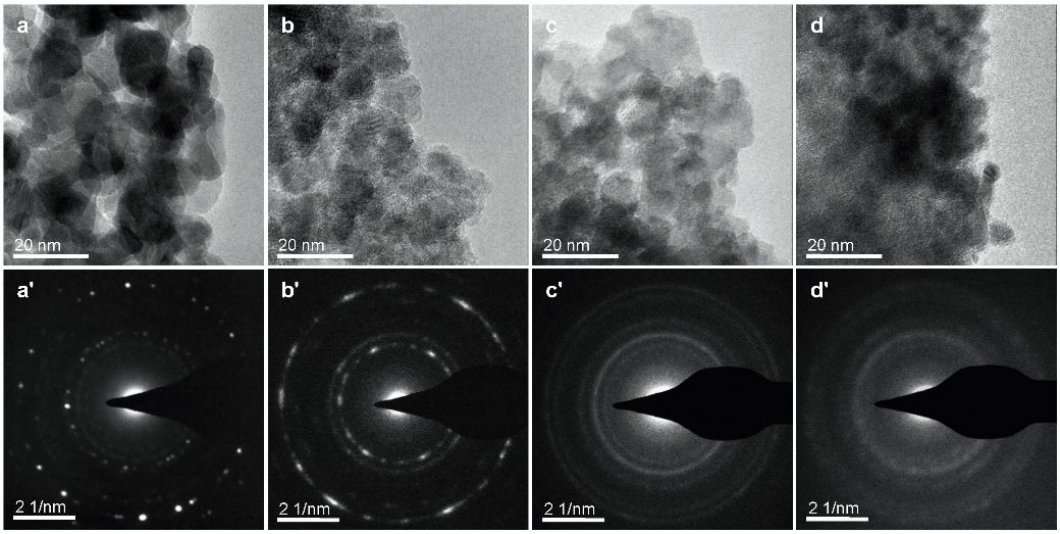

Figure S3. TEM images and SAED of samples $Co_{3-x}Ce_xO_4$, (a, a') pure Co_3O_4, (b, b') Ce/Co=3%, (c, c') Ce/Co=5% and (d, d') Ce/Co=8% (the percentage represents the molar ratio of Co and Ce in electrodeposition aqueous solution).

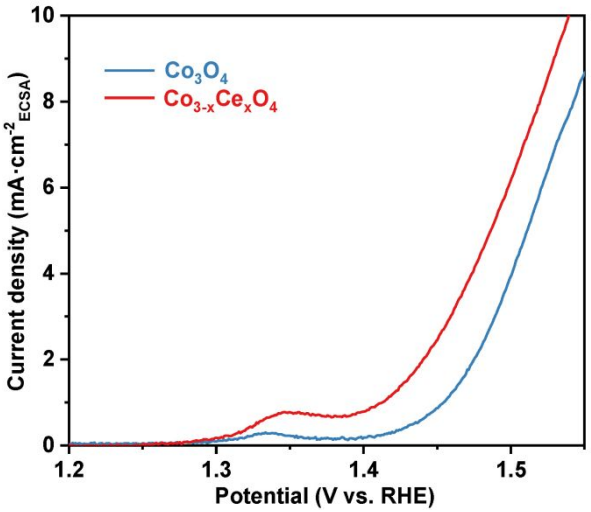

Figure S4. LSV curves for catalysts $Co_{1-x}Ce_xO_4$ and $Co_{1-x}Ce_xO_4$ performed on glass carbon without iR compensation.

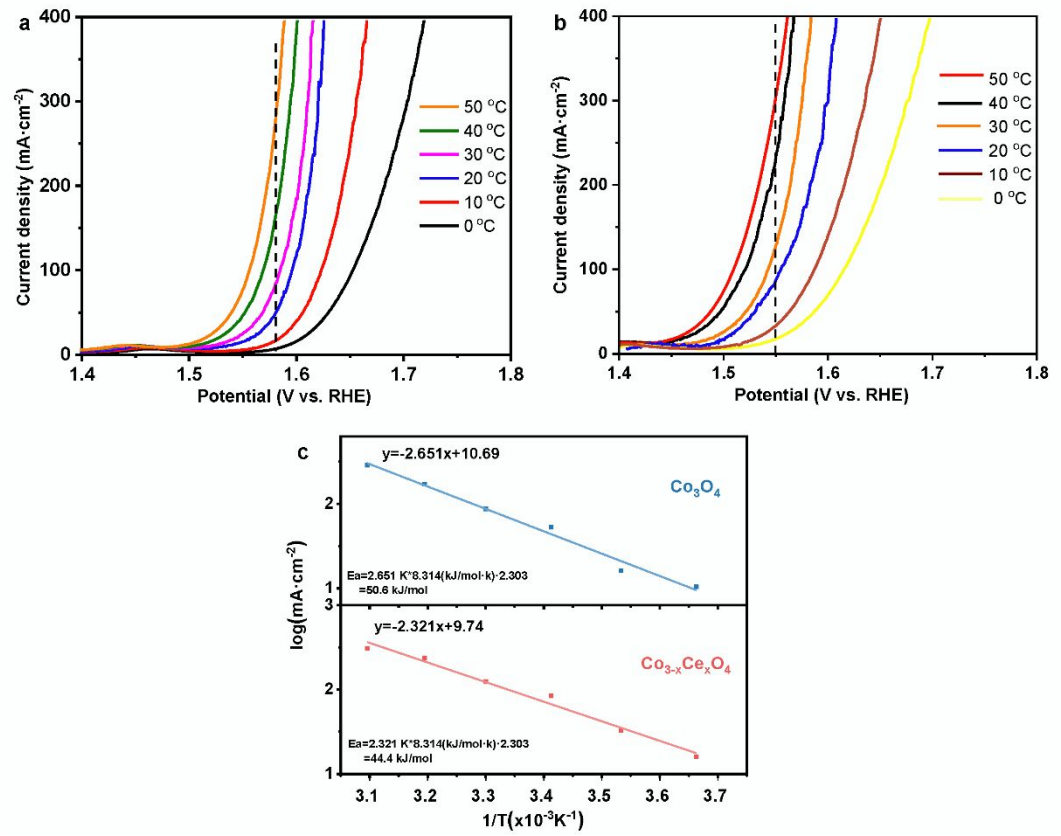

Figure S5. LSV curves of electrodes (a) NF/Co_3O_4 and (b) $NF/Co_{3-x}Ce_xO_4$ recorded under different temperatures. (c) Arrhenius plots of the Co_3O_4 and $Co_{3-x}Ce_xO_4$.

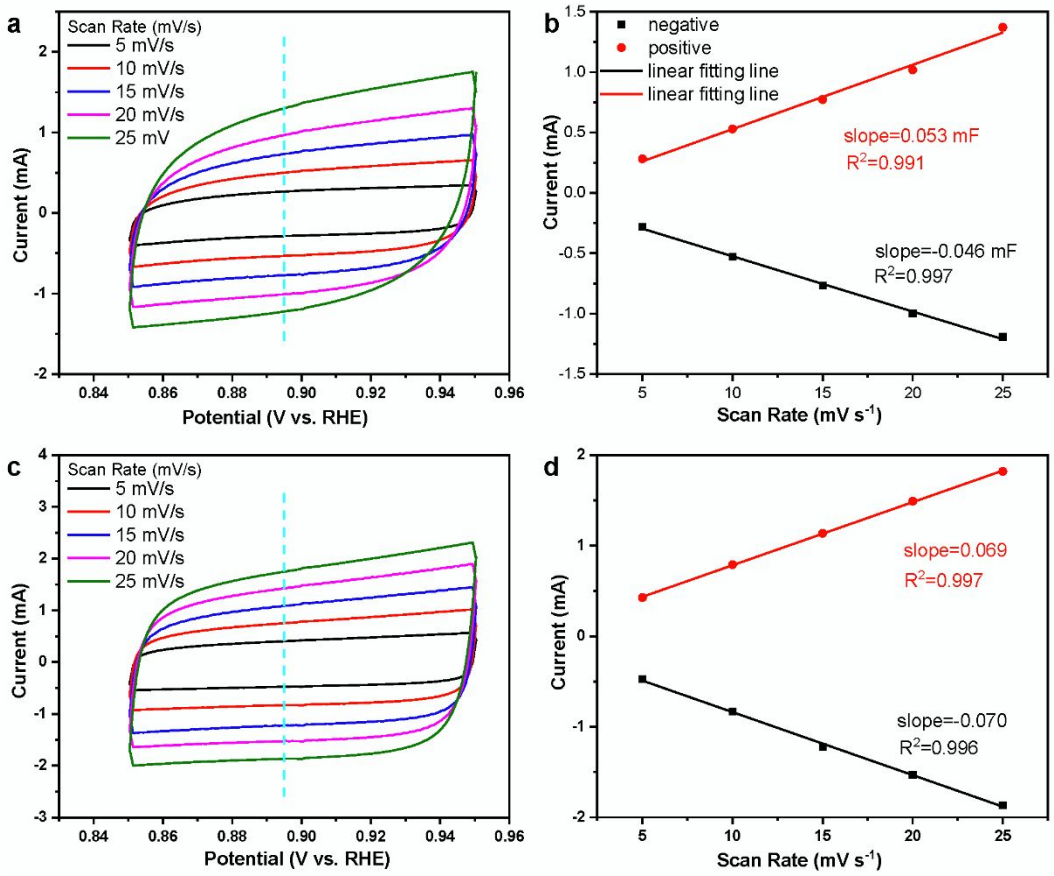

Figure S6. Cyclic voltammetry curves of electrodes (a) NF/Co_3O_4 and (c) NF/$Co_{3-x}Ce_xO_4$ at scan rate from 5 mV/s to 25 mV/s. Scan rate dependence of the current for electrodes (b) NF/Co_3O_4 and (d) NF/$Co_{3-x}Ce_xO_4$.

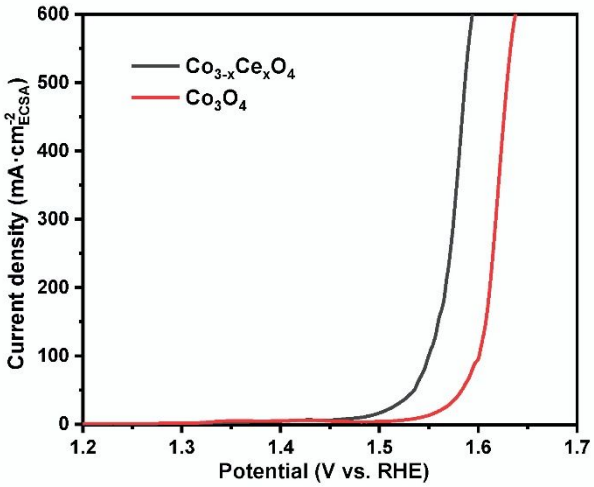

Figure S7. The ECSA corrected LSV curves for NF/Co_3O_4 and NF/$Co_{3-x}Ce_xO_4$.

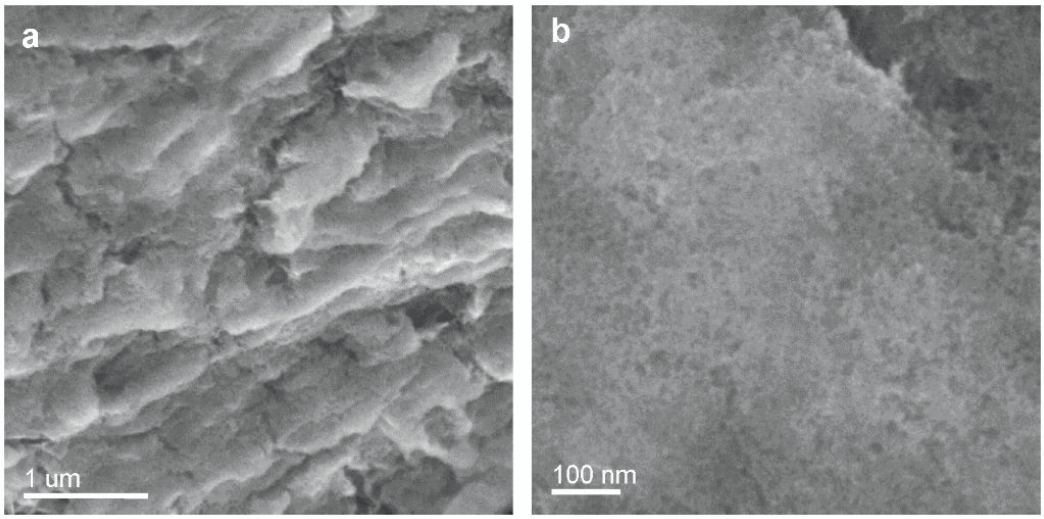

Figure S8. (a) Low- and (b) Large-magnification SEM of as-prepared Co_3O_4-CeO_2.

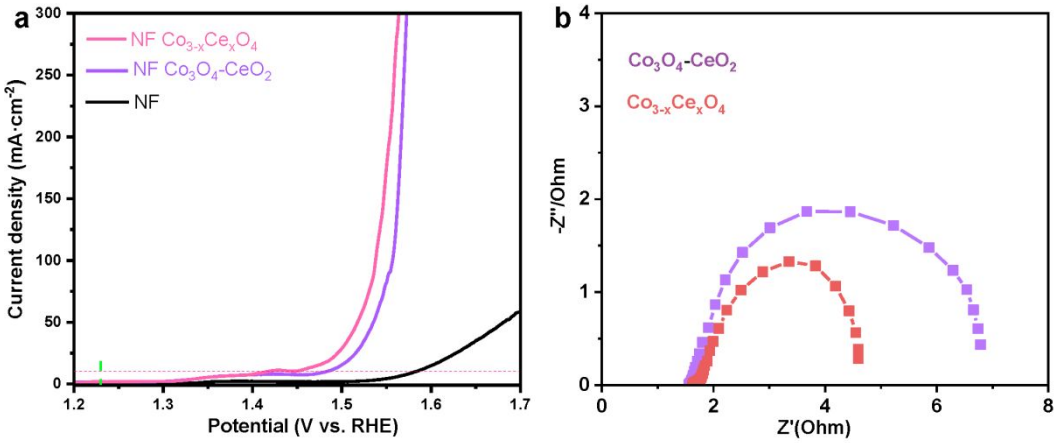

Figure S9. (a) LSV curves of electrode NF/$Co_{3-x}Ce_xO_4$ and NF/Co_3O_4-CeO_2 in O_2-saturated 1 M KOH electrolyte. (b) Comparison Nyquist plots for electrodes NF/Co_3O_4-CeO_2 and NF/$Co_{3-x}Ce_xO_4$.

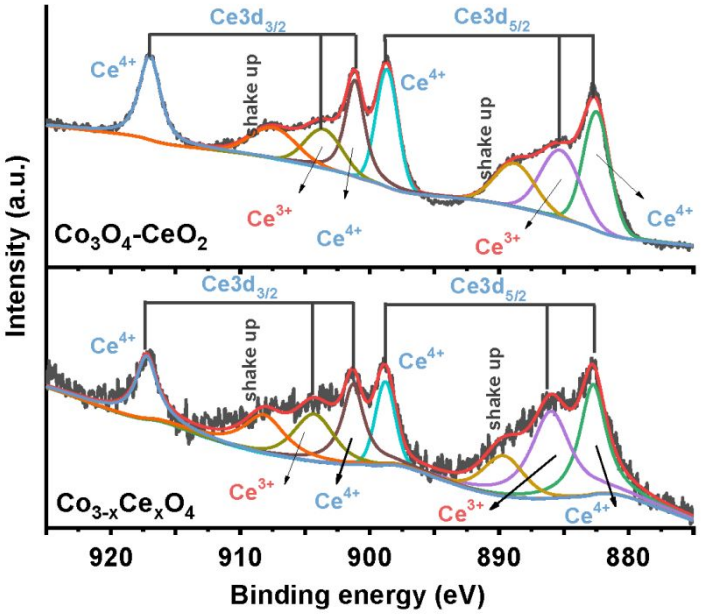

Figure S10. High-resolution XPS spectrum of Ce 3d for sample $Co_{3-x}Ce_xO_4$ and Co_3O_4-CeO_2

References

1. McCrory, C. C. L.; Jung, S.; Peters, J. C.; Jaramillo, T. F., Benchmarking Heterogeneous Electrocatalysts for the Oxygen Evolution Reaction. *J. Am. Chem. Soc.* **2013,** *135* (45), 16977-16987.

2. Xu, S.; Lv, C.; He, T.; Huang, Z.; Zhang, C., Amorphous film of cerium doped cobalt oxide as a highly efficient electrocatalyst for oxygen evolution reaction. *J. Mater. Chem. A* **2019,** *7* (13), 7526-7532.

3. Han, H.; Choi, H.; Mhin, S.; Hong, Y.-R.; Kim, K. M.; Kwon, J.; Ali, G.; Chung, K. Y.; Je, M.; Umh, H. N.; Lim, D.-H.; Davey, K.; Qiao, S.-Z.; Paik, U.; Song, T., Advantageous crystalline–amorphous phase boundary for enhanced electrochemical water oxidation. *Energy Environ. Sci.* **2019,** *12* (8), 2443-2454.